DOI: 10.1039/B907309B (Paper) *Lab Chip*, 2009, **9**, 3095-3099

Detection of prostate specific antigen with nanomechanical resonators

Philip S. Waggoner , Madhukar Varshney and Harold G. Craighead *

School of Applied and Engineering Physics, Cornell University, Ithaca, NY 14853, USA. E-mail: hgc1@cornell.edu ; Fax: +1 607-255-7658; Tel: +1 607-255-8707

Received 9th April 2009 , Accepted 31st July 2009

First published on 18th August 2009

Abstract

In this work, we use arrays of nanomechanical resonators to detect prostate specific antigen (PSA), a protein biomarker associated with prostate cancer. The surfaces of our very thin, trampoline-like devices are functionalised for immunospecific capture of PSA molecules, and the mass of bound material can be detected as a reduction in the resonant frequency. Fetal bovine serum was spiked with known concentrations of PSA, and in conjunction with a nanoparticle - based sandwich assay, concentrations as low as 50 fg mL^{-1}, or 1.5 fM, could be detected from the realistic samples. The presence of non-specific proteins in the serum did not significantly affect the sensitivity of our assay.

Introduction

There is increasing interest in improved medical diagnostics for personalised medicine and the early detection of disease. Ideally, these devices would feature high sensitivity, few false positive or negative readings, and the capability for large scale multiplexing. By monitoring a core set of biomarkers, the onset of common diseases or those to which the patient is hereditarily susceptible can be monitored, moving towards the ultimate of early detection. Such devices could supplant current tests and provide a better platform for individualised medicine.

Micro- and nanoelectromechanical systems (MEMS and NEMS) are one such technology that has the potential to achieve these goals, and many devices are currently being applied as biosensors for detection of infectious agents and disease biomarkers.[1–3] The small size and high sensitivity of MEMS and NEMS suggests that they are good candidates for miniaturised sensor systems and amenable to multiplexed detection through the use of arrays of devices that could be uniquely functionalised and feature on-chip redundancy for detection of each analyte. When used in sensing applications, the added analyte material can induce a surface stress, causing tip deflection in the case of static mode sensors, or change the mechanical properties or the mass of the devices, resulting in a resonant frequency shift for dynamic mode sensors.

In general, micro- and nanomechanical resonators can be modelled like harmonic oscillators with a resonant frequency, f, given by $f \propto (D\, m^{-1})^{-0.5}$, where D is the flexural rigidity and m is the resonator mass.[4] Changes in flexural rigidity, given by the product of material stiffness and the second moment of the cross-sectional area, have been observed for deposition of relatively stiff films on cantilevers.[5] However for the detection of soft biomolecules, flexural rigidity changes will likely be negligible.[6] In this regime, only changes in mass will dictate resonant frequency shifts. For small changes in mass, relative frequency shifts can be approximated as

$$\frac{\Delta f}{f} = -\frac{1}{2}\frac{\Delta m}{m} = -\frac{n\sigma}{2\rho t} \tag{1}$$

where $\Delta m/m$ is the ratio of added mass, Δm, to the initial resonator mass, m, n is 1 or 2 based on whether mass is added to one or both sides of the resonator, σ is the mass per unit area of the added material, and ρ and t are the density and thickness of the resonator, respectively. The frequency response, given by the quantity $\Delta f/f$, is used here rather than absolute frequency shift because it is unaffected by variations in the initial frequency, f, from device to device due to slight differences in the fabricated structures. From Eqn (1), it is evident that thinner and less dense resonators make the best mass sensors.

Resonators used in this work are trampoline shaped, unlike the traditional cantilever geometry found ubiquitously in the literature; an SEM micrograph of the arrayed devices is shown in Fig. 1(a). Recent work has demonstrated that cantilevers are not always the most sensitive geometry and that trampoline-like resonators have a relatively uniform frequency response for the mass of bound material located anywhere across its central paddle because of its unique resonant mode shape.[6] Such a uniform response across much of the sensing area would be desirable for the detection of dilutely added materials, as it would reduce variations from device to device caused by randomly distributed binding events. This effect motivated the use of paddlever resonators in recent work for the detection of prion proteins,[7] and trampolines represent the next logical step in improving the uniformity of the positional mass sensitivity.

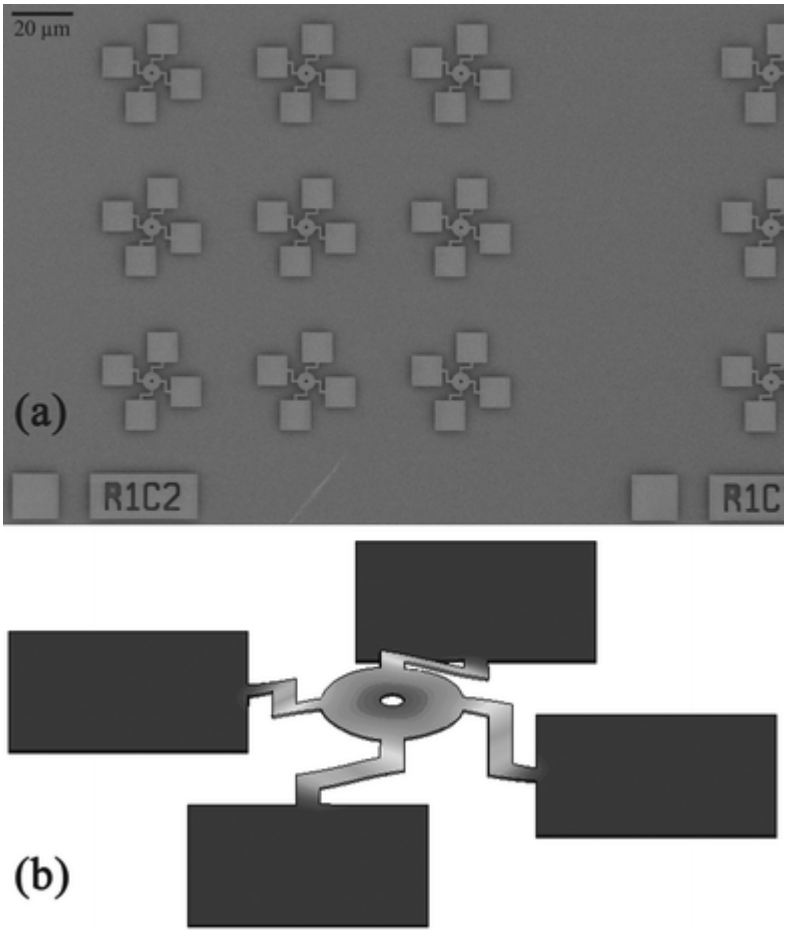

Fig. 1 (a) SEM micrograph of 3 × 3 arrays of trampoline resonators with 50 µm between adjacent devices. The centre area of each device measures 6 µm in diameter, with a 1 µm dia. hole at the centre for etching purposes. (b) Image obtained using finite element analysis depicting the displacement of the device in the fundamental resonant mode.

The trampoline centre has a diameter of 6 μm, and the support arms are 1 μm wide. These flexible supports allow the centre to move in and out of plane with fairly constant amplitude and help to concentrate the majority of the device sensing area in the region most sensitive to mass loading, the central paddle.[6] This motion is depicted in Fig. 1(b), showing the extent of trampoline displacement for the fundamental resonant mode, which is used in this work. In addition, the large surface area of these devices, ~54 μm^2, is significantly greater than that of the previously used 4 μm long paddlevers, ~30 μm^2,[7] or cantilevers of the same length, ~8 μm^2, increasing the probability of capturing analytes at extremely low concentrations, which may improve sensitivity.

As a model biomarker for our resonant sensors, we use prostate specific antigen (PSA), a clinically monitored protein used in screening tests for prostate cancer.[8] PSA is a normally produced protein found at a high concentration in seminal fluid. Elevated concentrations of PSA in the blood are associated with a higher risk for prostate cancer and may indicate damage of the prostate tissue, allowing PSA to escape into circulation.[9] While PSA can be found in its free form, it is more common for it to be complexed with enzymes or other molecules, such as α1-chymotrypsin, α1-protease inhibitor, or α2-macroglobulin. At this time, sensitivity to total PSA (free and complexed) concentrations in the range of 2 to 10 ng mL^{-1} are required, as there is elevated risk for prostate cancer at these concentrations, while for free PSA the clinically relevant concentrations range from ~0.5 to 1.2 ng mL^{-1} (15–36 pM).[8]

When PSA is found at or above these concentrations, a biopsy is often required as the next step to assess whether the increased concentration is associated with prostate cancer or another condition such as benign prostate hyperplasia. However, many such biopsies are negative for cancer; it has been suggested that monitoring the percentage of free to complexed PSA may be more sensitive and also avoid unnecessary biopsies by helping to discern between benign and malignant conditions.[10] With improved sensitivity to PSA levels in serum, its concentration could be tracked over a long period of time at lower concentrations, and increased risk could be gauged from case to case by personal baselines and trends rather than approximate, age-based cut-off guidelines.

Several groups have used MEMS or NEMS sensors in order to detect PSA. Microcantilevers have been used in static deflection mode to detect the surface stress associated with PSA binding to an antibody-coated surface, demonstrating sensitivity to 0.2 ng mL^{-1}.[11] Similar devices were used in a two-dimensional array of sensors for PSA through surface-stress induced deflection, detecting 1 ng mL^{-1}.[12]

While predominantly used as mass sensors, some have suggested that dynamic, resonant MEMS or NEMS devices could also respond to surface stresses resulting from PSA binding. Hwang *et al.* reported

PSA detection of 1 ng mL^{-1} using relatively large microcantilever resonators operated in liquid, stating that the frequency shifts arose from a combination of mass-loading effects and a compressive surface stress.[13] Recent work claims that PSA can be detected solely through frequency shifts due to surface stress, down to a level of 10 pg mL^{-1}, or even down to 1 pg mL^{-1} if a secondary sandwich antibody is used.[14] However, the calculated surface stresses are much larger than previously reported; for instance, a PSA concentration of 1 ng mL^{-1} produced a compressive surface stress of ~40 mN m^{-1}, in contrast with the experiments discussed above in Ref. 11 and 12, where compressive surface stresses of approximately 4 and 2 mN m^{-1} were found, respectively. In addition, Lachut and Sader have questioned the validity of axial-force models like that used in Ref. 14 to relate surface stress to resonant frequency, stating that such models violate Newton's third law.[15]

Prostate specific antigen has a small molecular weight of ~33 kDa or roughly 55 zg (10^{-21} g). At low concentrations, it is unlikely that the number of PSA bound to resonators would have sufficient mass to produce a detectable frequency shift. However, PSA detection has been demonstrated in liquid at a concentration of 10 ng mL^{-1} using a mass-sensitive, resonant cantilever.[17] A technique of secondary mass labelling has been demonstrated in order to overcome this issue, and has been used for the detection of nucleic acids[16] and proteins[7] with mechanical resonators. In these secondary labelling systems, an additional biorecognition molecule is used to tether a heavy mass to analytes already bound to the resonator surface. Not only is this important for increasing the sensitivity of resonant sensors at low concentrations, but it also improves their specificity, due to the use of an additional biorecognition molecule for the analyte. This ability to detect dilutely-bound analytes is one advantage resonant MEMS and NEMS have over similar surface stress cantilever sensors, as recent studies have suggested that there is a percolation threshold requiring a network of binding events to collectively produce a surface stress that can bend a cantilever.[18]

For any biomolecular sensing platform, it is important that its sensitivity be assessed using realistic samples, such as blood serum, urine, or saliva, as sensors applied in the medical field would face these solutions every day. The primary issue that arises when working with serum rather than standard buffer solution is the non-specific binding of other background proteins or biomolecules to the sensor surface. This is typically assumed to sterically block specific binding sites and reduce the amount of captured analyte. In addition, non-specifically bound materials can alter the signals of both mass and surface stress sensors, potentially reducing or even exaggerating measured signals that should be associated with only specific interactions. One recent study using micromechanical resonators to detect PSA has tried to combat this with using prolonged washing after serum has been introduced to the devices, which

appeared to remove a large part of the non-specifically bound material.[19] In serum, they observed signal reduction and a detection limit of 100 pg mL^{-1}, however, no explicit data from control measurements was shown, which is required to determine the effect of the background media on the sensors and the detection limit.

In this work we use a sandwich assay-based, secondary mass labelling technique in order to detect PSA. Arrays of trampoline resonators were functionalised with capture antibodies specific to PSA, and a second antibody was used to specifically tether nanoparticle mass labels to PSA molecules attached to the devices. These devices demonstrated PSA detection from undiluted serum at concentrations ranging from 50 ng mL^{-1} down to 50 fg mL^{-1}, or 1.5 fM.

Experimental procedure

Resonator fabrication

Devices were fabricated using standard lithographic techniques for surface micromachining. Clean silicon wafers were thermally oxidised to form a 1.8 μm thick sacrificial layer of silicon dioxide. Following oxidation, a 90 nm thick layer of low stress silicon nitride was grown on the wafer. Resonator designs were then patterned using photolithography and an anisotropic, CF_4-based reactive ion etch chemistry. Next, chips containing thousands of arrayed resonators each were diced from the wafer. Device chips were then etched with hydrofluoric acid in order to remove the sacrificial oxide layer so that the resonators would be free to move. The hole in the device centre was required to etch the silicon dioxide beneath the trampoline and fully release the devices. Critical point drying was not required at any point in the device fabrication or surface modification because the sacrificial oxide layer was sufficiently thick as to avoid stiction phenomena.

Device chips were loaded into a small vacuum chamber mounted to a motorised stage, and the resonant frequencies were measured in vacuum at pressures <10^{-3} Torr. The resonators were mechanically excited into resonance by mounting them on an external piezoelectric element driven at the resonant frequencies of devices. Clean, freshly released devices had resonant frequencies of roughly 2.2 MHz and quality factors of ~6000. A HeNe laser (632.8 nm) was focused at the centre of the trampolines and used to interferometrically detect device resonance. Laser power delivered to each device was kept at a minimum (typically on the order of 50 μW) in order to minimise heating effects. The reflected signal was collected using a fast photodetector and read out using a spectrum analyser. A custom-built graphic user interface program has been developed to control the stage and the spectrum analyser, allowing automated readout

of an array of devices in minutes. In this work, frequency shifts were measured using many devices from different arrays on each chip, and the average frequency responses were considered, while error bars are determined by the standard deviations.

Surface chemistry

In order to specifically capture PSA on resonators and detect their presence, a sandwich immunoassay was performed on device surfaces. After HF release, chips were cleaned for 30 minutes in a 2:1 piranha solution (concentrated sulfuric acid to 30% hydrogen peroxide) and then for 30 minutes in an oxygen plasma. Devices were functionalised with 3-aminopropyltriethoxysilane (APTES, Sigma, 99%) overnight (~16 hours) using a 10% solution in dry toluene (Sigma, 99.8%) in a moisture-free environment. Following silanisation, the device chips were washed in a series of acetone, isopropanol, and water, and then soaked in DI water for 15 minutes on an orbital shaker in order to remove excess APTES. Surface modification continued by soaking chips in a 5% solution of gluteraldehyde (Sigma, 50%) in borate buffer for 2 hours, serving as a covalent cross-linker molecule between the amine groups on the silanised surface and antibodies. Following this and all subsequent steps, device chips were washed twice in purified DI water on an orbital shaker operating at 95 RPM. Each washing step was two minutes long, and fresh water was used between washes. This washing was performed in water rather than buffer in order to prevent buffer salt crystals which form abundantly on the surface if buffer is allowed to dry on the devices, rendering the sensors effectively useless.

Next, affinity-purified, polyclonal goat antibodies for human free PSA were immobilised on the surface during a one hour incubation using an antibody concentration of 50 µg mL^{-1}. Unreacted gluteraldehyde was then quenched by immersing the chips in 50 mM solution of glycine for 30 minutes. A blocking step was performed for 15 minutes using a 1% solution of bovine serum albumin (BSA) in phosphate buffered saline (PBS) that had been filtered through a 0.2 µm pore filter. Free PSA (>98% pure, human) was then spiked into undiluted fetal bovine serum (FBS, HyClone, Thermo Scientific) at concentrations ranging from 50 fg mL^{-1} to 50 ng mL^{-1} and incubated on the devices for one hour. Control chips were incubated with FBS containing no PSA. All FBS was filtered through 0.2 µm filter prior to use. Following another 15 minute blocking step in 1% BSA, monoclonal mouse antibodies to human free PSA (epitope 1) were used as the secondary antibody in the sandwich assay and incubated on devices at a concentration of 50 µg mL^{-1} in PBS for one hour. Both of the antibodies as well as the PSA were purchased from Meridian Life Science, Inc. (Cincinnati, OH).

Magnetic nanoparticles coated in goat anti-mouse IgG antibodies (R&D Systems, Minneapolis, MN) were used to bind to the secondary mouse antibodies. The nanoparticles measure roughly 100–150 nm in diameter, and correspondingly have masses on the order of 1 fg. Prior to incubation with nanoparticles, a 15 minute blocking step was again performed. Finally, a 1:50 dilution of nanoparticles was prepared in the 1% BSA blocking solution and incubated on chips for 90 minutes, followed by another washing step. The chips were dried using a stream of nitrogen before loading in vacuum and measuring resonant frequencies before and after incubation with nanoparticles.

Results and discussion

In order to assess the effect of fetal bovine serum on the assay, we tested the detection of 50 pg mL^{-1}PSA diluted in PBS and serum. For both media, a control chip was used with no spiked PSA present in order to determine the background effects of the buffer and serum. Our results are shown in Fig. 2, where only a small increase in background was observed for the chips exposed to FBS. This corresponded with a slightly decreased difference between control and sample, however, the two frequency responses were within error of each other. These results indicate that our blocking and washing procedures are effective and that the detection of PSA in the presence of serum does not strongly affect the frequency responses due to nanoparticle labels later in the assay protocol.

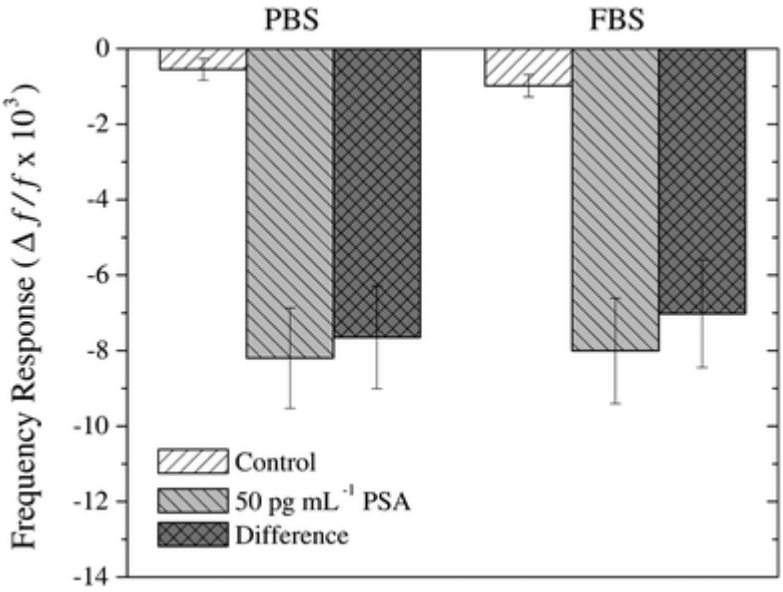

Fig. 2 Comparison of resonant frequency responses in the detection of PSA at 50 pg mL^{-1} in PBS buffer and fetal bovine serum (FBS). While a small amount of non-specific binding is evident from the increased FBS control, the two differential signals are still within error of each other.

Additional PSA concentrations ranging from 50 pg mL^{-1} to 50 fg mL^{-1} were tested, and the frequency responses due to nanoparticle addition are shown in Fig. 3. In order to compare the responses from experiments performed on different days, the control frequency shift was subtracted from all other shifts from that day in order to determine and compare the portions of the frequency shifts associated with mass specifically added to resonators. This differential shift takes into account the variations in environmental conditions, surface functionalisation, and nonspecific binding from day to day. The control frequency responses were typically ranged from 0 to -1×10^{-3}. We attribute this variability to changes in environmental conditions that occur between the frequency readings. To illustrate, several controls from the above data are shown in the inset of Fig. 3. The 50 fg mL^{-1} frequency shift was found to be significantly different from a null shift ($P < 0.0005$) using a one-tailed, student's t-test. Similarly, the frequency shifts for all concentrations were found to be significantly different from neighbouring concentrations ($P < 0.001$).

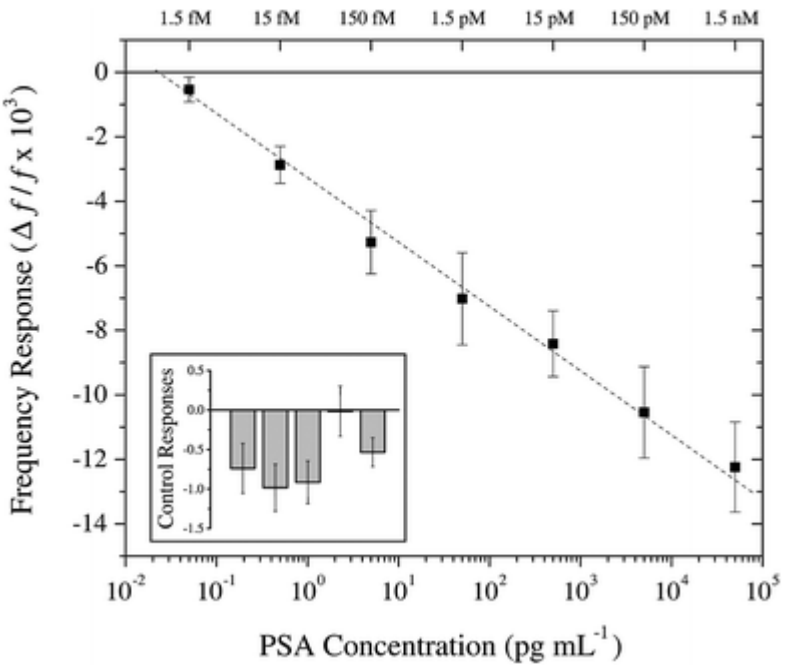

Fig. 3 Frequency response of resonant sensors due to the addition of nanoparticles for different PSA concentrations, demonstrating a concentration sensitivity of 50 fg mL^{-1} ($P < 0.0005$). The inset shows control responses observed during the tests performed at different concentrations, demonstrating consistent but slightly varying background signals due to variations in non-specific binding and environmental conditions from day-to-day.

To illustrate nanoparticle binding, SEM micrographs were taken of the devices, and representative images at several concentrations are shown in Fig. 4. For lower concentrations of PSA, fewer nanoparticles were bound to the resonators. We also note that nanoparticles should also be bound to the bottom of the trampoline, as all device surfaces were functionalised. In this case, the assumption of mass addition as a uniform layer breaks down, and the nanoparticles behave essentially as point masses. From the low binding densities of nanoparticles at these concentrations, it becomes evident that these trampoline resonators are more sensitive than previously used paddlever resonators.[5] If the same nanoparticle binding density were present on the smaller paddlever devices, they would likely have fewer nanoparticles bound to them at such low PSA concentrations, resulting in a reduced detection limit even if they were of the same thickness. On the other hand, if a cantilever with the same surface area as our circular trampolines were used, roughly the same number of nanoparticles would be bound to it, but the highly non-uniform frequency response of cantilevers along their length would likely increase the standard deviations for each concentration by a significant amount, also reducing sensitivity.[6]

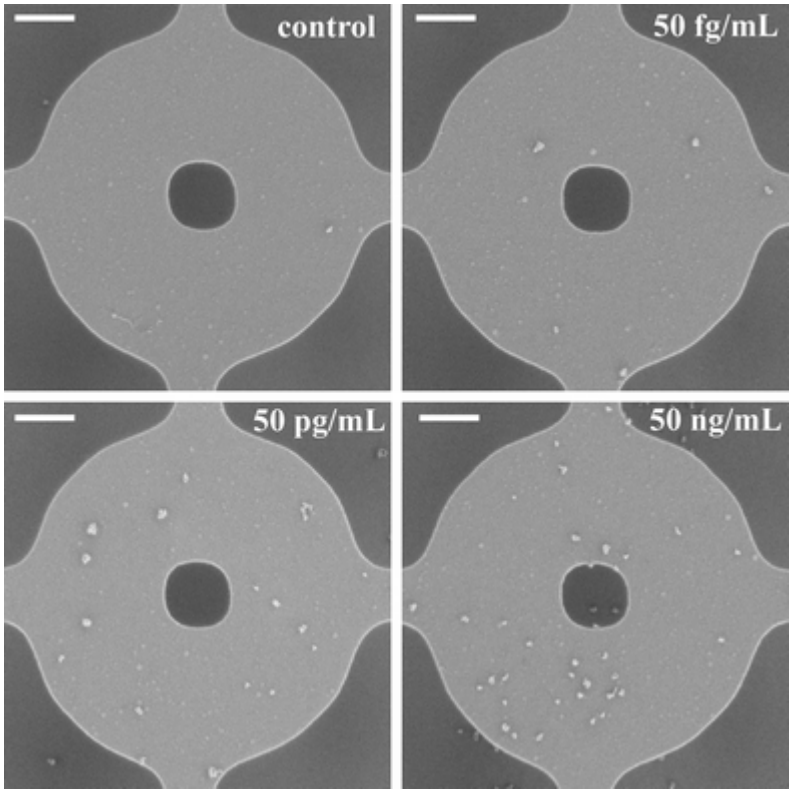

Fig. 4 Representative SEM images of trampoline resonators showing that the number of nanoparticles bound to devices scales with PSA concentration. Scale bar represents 1 μm.

There are several ways in which the present assay could be improved. First, in order to achieve high quality factor resonances of the devices, all frequency measurements are taken in vacuum, which presents some challenges to use in a clinical laboratory setting. While it is unlikely that our nanomechanical resonant sensors and similar devices could be used with high sensitivity in liquid due to the very strong effects of viscous damping, it would be feasible with proper optimization to measure the resonant frequencies of some devices in air, where quality factors on the order of 100–1000 have been demonstrated.[20–22] In addition, the standard deviations shown in Fig. 3, representing the device-to-device variability of the frequency shift, are affected by several factors, including nonspecific binding and the nature of nanoparticles used. For instance, the use of nanoparticles with reduced polydispersity would decrease the variations in frequency shift due to variable nanoparticle size and composition. In addition, further optimizing the blocking and washing protocols could improve the uniformity of the assay and reduce the standard deviations. Also, device sensitivity may be improved by increasing the concentration of nanoparticles in order to increase the number bound for each PSA concentration using the same incubation time, as long as they do not nonspecific bind and increase the control frequency shifts proportionately.

Conclusions

Clinically relevant concentrations of prostate specific antigen were detected from undiluted fetal bovine serum using nanomechanical trampoline resonators at concentrations ranging from 50 fg mL^{-1} to 50 ng mL^{-1}, or 1.5 fM to 1.5 nM. We also note that the flexibility of these sensors is limited only by the availability of specific biorecognition layers and functionalisation techniques. The high sensitivity of these robust resonator arrays, in addition to their small size and versatility, suggests that they will find use in many applications, including miniaturised sensors and multiplexed detection systems.

Acknowledgements

This project was funded in part by Intel Research. We would like to thank C. P. Tan for helpful discussions. Device fabrication was performed at the Cornell NanoScale Facility, a member of the National Nanotechnology Infrastructure Network, which is supported by the National Science Foundation.

References

1. N. V. Lavrik, M. J. Sepaniak and P. G. Datskos, *Rev. Sci. Instrum.*, 2004, **75**(7), 2229–2253 CrossRef CAS .
2. P. S. Waggoner and H. G. Craighead, *Lab Chip*, 2007, **7**, 1238–1255 RSC .
3. J. Fritz, *Analyst*, 2008, **133**, 855–863 RSC .
4. W. Weaver, Jr., S. P. Timoshenko, D. H. Young, *Vibration Problems in Engineering*, Wiley Interscience, New York, 5th edn, 1990 Search PubMed .
5. K. E. Petersen and C. R. Guarnieri, *J. Appl. Phys.*, 1979, **50**(11), 6761–6766 CrossRef CAS .
6. P. S. Waggoner and H. G. Craighead, *J. Appl. Phys.*, 2009, **105**, 054306 CrossRef .
7. M. Varshney, P. S. Waggoner, C. P. Tan, K. Aubin, R. A. Montagna, and H. G. Craighead, *Anal. Chem.*, 80, pp. 2141–2148 Search PubMed .
8. P. Wu, H. Koistinen, P. Finne, W.-M. Zhang, L. Zhu, J. Leinonen and U.-H. Stenman, *Adv. Clin. Chem.*, 2006, **41**, 231–261 Search PubMed .
9. S. P. Balk, Y.-J. Ko and G. J. Bubley, *J. Clin. Oncology*, 2003, **21**(2), 383–391 CrossRef CAS .
10. W. J. Catalona, P. C. Southwick, K. M. Slawin, A. W. Partin, M. K. Brawer, R. C. Flanigan, A. Patel, J. P. Richie, P. C. Walsh, P. T. Scardino, P. H. Lange, G. H. Gasior, K. G. Loveland and K. R. Bray, *Urology*, 2000, **56**(2), 255–260 CrossRef CAS .
11. G. Wu, R. H. Datar, K. M. Hansen, T. Thundat, R. J. Cote and A. Majumdar, *Nat. Biotechnol.*, 2001, **19**, 856–860 CrossRef CAS .
12. M. Yue, J. C. Stachowiak, H. Lin, R. Datar, R. Cote and A. Majumdar, *Nano Lett.*, 2008, **8**(2), 520–524 CrossRef CAS .
13. K. S. Hwang, J. H. Lee, J. Park, D. S. Yoon, J. H. Park and T. S. Kim, *Lab Chip*, 2004, **4**, 547–552 RSC .
14. S. Lee, K. S. Hwang, H. Yoon, D. S. Yoon, S. K. Kim, Y. Lee and T. S. Kim, *Lab Chip*, 2009 10.1039/b902922b .
15. M. J. Lachut and J. E. Sader, *Phys. Rev. Lett.*, 2007, **99**, 206102 CrossRef .
16. M. Su, S. Li and V. P. Dravid, *Appl. Phys. Lett.*, 2003, **82**(20), 3562–3564 CrossRef CAS .
17. C. Vancura, Y. Li, J. Lichtenberg, K. Kirstein, and A. Hierlemann, 2007, 79, pp. 1646–1654.
18. J. W. Ndieyira, M. Watari, A. D. Barrera, D. Zhou, M. Vogtli, M. Batchelor, M. A. Cooper, T. Strunz, M. A. Horton, C. Abell, T. Rayment, G. Aeppli and R. A. McKendry, *Nat. Nanotechnol.*, 2008, **3**, 691–696 Search PubMed .
19. K. S. Hwang, H. K. Jeon, S.-M. Lee, S. K. Kim and T. S. Kim, *J. Appl. Phys.*, 2009, **105**, 102017 CrossRef .
20. J. W. M. Chon, P. Mulvaney and J. E. Sader, *J. Appl. Phys.*, 2000, **87**, 3978 CrossRef CAS .

21. J. F. Vignola, J. A. Judge, J. Jarzynski, M. Zalalutdinov, B. H. Houston and J. W. Baldwin, *Appl. Phys. Lett.*, 2006, **88**, 041921 CrossRef .
22. P. S. Waggoner, C. P. Tan, L. Bellan and H. G. Craighead, *J. Appl. Phys.*, 2009, **105**, 094315 CrossRef .